

CHROM. 20 673

## SPLIT PEAKS IN NON-LINEAR CHROMATOGRAPHY AND THEIR EFFECT ON SAMPLE THROUGHPUT IN LARGE SCALE SEPARATIONS

JAMES L. WADE\* and PETER W. CARR\*

*Department of Chemistry, Smith and Kolthoff Halls, University of Minnesota, Minneapolis, MN 55455 (U.S.A.)*

(Received April 15th, 1988)

---

### SUMMARY

The origin and mathematical properties of the split peak phenomenon are described for both linear and non-linear elution conditions. Through a series of computer calculations, the theoretical behavior of split peaks is predicted for a wide variety of conditions where chemical adsorption, as opposed to solute mass transfer, is the rate-limiting adsorption step. Our results, which derive from the fundamental solution of the non-linear chromatographic equations with an impulse input [ $\delta(t)$ ], are found to be in excellent agreement with the recent numerical simulations of Hage and Walters. The fraction of solute eluting at the dead volume ( $f$ ) is found to be a complex function of both the flow-rate and the amount injected ( $C_0$ ). Although it is theoretically possible to use the split peak mass to derive values for the adsorption rate constant and the density of binding sites, this methodology is difficult and time-consuming to apply. Split peak theory may be useful, however, in engineering design computations where it is desired to maximize solute throughput, yet keep the non-retained fraction below a certain percentage of the total mass of solute applied to the column. Universal working curves for this purpose are presented and discussed, and the optimum throughput is found for each of several specified split peak fractions.

---

### INTRODUCTION

One of the more curious phenomena in chromatography is the so-called "split peak". These occur when adsorption is so slow, or the density of binding sites is so small, that a significant fraction of the solute may traverse the length of the column without adsorbing even once<sup>1</sup>. The probability of a solute making this passage is enhanced by higher flow-rates, and is completely independent of the rate of solute desorption from the stationary phase; the amount of solute eluting at the dead volume depends only on its probability of *adsorbing* during its residence in the column.

Split peaks are found almost exclusively in protein and affinity chromatography, where both the solute and the immobilized ligand molecules tend to be large, and

---

\* Current address: Hercules Research Center, Hercules Incorporated, Wilmington, DE, 19894, U.S.A.

adsorption kinetics and mass transfer tend to be slow. Split peaks are not useful in quantitative analysis or in preparative scale work; indeed, they are undesirable artifacts. They have been used, however, to make physico-chemical measurements; their mass—a convenient and precisely measurable quantity—is directly related to the density of binding sites on a particular adsorbent, as well as to the adsorption kinetics of these sites<sup>2,3</sup>.

Sportsman and Wilson<sup>2</sup> were the first to make use of this fact in measuring the rate of formation of an antigen-antibody complex<sup>2</sup>. Recently, Hage *et al.*<sup>3</sup> used split peaks in an elegant study of the immobilization-dependent adsorption kinetics of Protein A<sup>3</sup>. They found that the chemical procedures used to immobilize the ligand had a significant effect on its adsorption kinetics. Their method of relating split peak mass to adsorption kinetics was, like Sportsman's, based on the assumption of linear ("infinite dilution") conditions. This has two undesirable consequences. First, linear elution conditions are all but unattainable in immobilized protein chromatography because ligand densities are simply too low; a detection system would not be able to measure precisely an "infinitely dilute" concentration of solute. Hence, experimental results need to be extrapolated to infinite dilution so that the linear theory may be properly applied. A further drawback to applying linear theory is that the density of binding sites must be known *a priori* in order to measure the adsorption rate constant. Each of these factors increases the number of experiments to be performed, thus diminishing the precision of the results.

Split peaks were first described in a theoretical way by Giddings and Eyring<sup>1</sup>, long before they were observed in affinity chromatography. In providing a stochastic description of the chromatographic process under linear conditions, they found that there was a finite probability, given sufficiently extreme chromatographic conditions, that an otherwise retained solute could travel the length of a column without adsorbing. DeLisi *et al.*<sup>4</sup> also examined linear split peak theory, and discussed its significance. It was only recently, however, that Hage and Walters<sup>5</sup> examined non-linear split peak theory for the first time. They used a finite element numerical analysis scheme to quantitatively simulate split peak behavior under two sets of conditions: (1) adsorption being limited by the rate of solute diffusion through the stagnant fluid, and (2) adsorption being limited by the rate of chemical adsorption. They also developed guidelines whereby non-linear effects in split peak behavior can be minimized, and "infinite dilution" behavior extrapolated from non-linear data.

In this article, we will examine the mathematical origin and behavior of split peaks in the adsorption-limited case, and discuss the difficulty of applying the appropriate theory to make physico-chemical measurements. If the physical parameters of a system have been accurately obtained by alternative means, however, split peak theory can prove to be useful. This is demonstrated by design calculations which provide a quantitative guide to optimizing solute throughput at a specified split peak fraction.

## THEORY

The non-linear system of equations which describes column overload under non-ideal conditions was solved for a delta function input to yield the following concentration-time relationship at the column exit<sup>6</sup>:

$$\frac{C}{C_0} = \left[ \frac{1 - \exp(-\gamma KC_0)}{\gamma KC_0} \right] \left[ \frac{[\gamma \sqrt{(k'/y)} I_1(2\gamma \sqrt{k'y}) + \delta(y)] \exp(-\gamma k' - \gamma y)}{1 - T(\gamma k', \gamma y) [1 - \exp(-\gamma KC_0)]} \right] \quad (1)$$

$$\frac{\tilde{q}}{C_0} = \left[ \frac{1 - \exp(-\gamma KC_0)}{\gamma KC_0} \right] \left[ \frac{\gamma k' I_0(2\gamma \sqrt{k'y}) \exp(-\gamma k' - \gamma y)}{1 - T(\gamma k', \gamma y) [1 - \exp(-\gamma KC_0)]} \right] \quad (2)$$

where:  $\tilde{q} = \varepsilon q$ ;  $\gamma = k_a t_0$ ;  $k' = (k_a/k_d) S_0 \varepsilon$ ;  $KC_0 = (k_a/k_d) C_0$ ;  $y = (t/t_0) - 1$ ;  $T(u, v) = \int_0^u e^{-t} I_0(2\sqrt{vt}) dt$ . The computation of the T function, a Bessel function integral, has been discussed elsewhere<sup>6</sup>. In the above equations,  $C$  and  $q$  represent the concentration of solute in the mobile and stationary phases, respectively, and  $C_0$  represents the quantity of solute injected or, in mathematical parlance, the “strength” of the delta function input. This may be computed in the following manner:

$$C_0 = \frac{V_p}{V_0} C_p \quad (3)$$

$C_p$  is the concentration of solute in a very narrow injection pulse,  $V_p$  is the volume of that pulse, and  $V_0$  is the dead volume of the column. The adsorption/desorption rate constants,  $k_a$  and  $k_d$ , are chemical constants; that is, we are assuming that a chemical process, as opposed to a mass transfer process, is the rate-limiting sorption step.  $S_0$  is the concentration of binding sites on the adsorbent,  $\varepsilon$  is the porosity ratio, and  $t_0$  is the dead time of the column. All symbols are summarized in the symbols section.

The profile of a non-linear chromatographic peak is fully described by three dimensionless groups,  $\gamma$ ,  $k'$ , and  $KC_0$ , and dimensionless time,  $y$ . Time is rendered dimensionless in this way in order to incorporate the initial condition that the column be empty; that is, nothing may elute prior to the dead time. This time “shift” is also essential to linearizing, and hence solving, the non-linear set of equations via the Thomas transformation<sup>7,8</sup>.

The shifted time variable does, however, present a problem when solving the non-linear chromatographic equations for an impulse input. This problem arises because the solute is introduced onto the column as an infinitely high, infinitely narrow pulse at *time equal to zero*; this is in contradiction to our condition, implicit in the time “shift”, that the column be initially devoid of all solute. Thus it is not surprising that while eqn. 1 accurately describes the profile of the retained peak, the delta function term (at  $y = 0$ ) does not correctly predict the split peak mass, except under linear conditions.

This is an unfortunate, but necessary, consequence of solving the non-linear system of equations with a boundary condition that is infinitely discontinuous at time equal to zero. In the derivation of eqns. 1 and 2, it was necessary to develop an expression for the boundary condition at  $y = 0$ , and because of the delta function, it was necessary to take the limit as  $y$  approached zero<sup>6</sup>. Taking the limit from the positive direction yields solutions which are trivially equal to zero, while taking the limit from the negative direction yields the solutions in eqns. 1 and 2. It can be shown, however, that when integrated over time, eqn. 1 will yield a mass which is less than or equal to unity, and the “missing mass” is, in fact, the correct split peak mass. This is the approach we have taken to compute split peak mass in our numerical calculations.

## NUMERICAL CALCULATIONS

Two sets of computer calculations were carried out. In the first, the three chromatographic parameters ( $\gamma$ ,  $k'$ , and  $KC_0$ ) were varied over a wide range, and theoretical peaks with approximately 160 points were generated. Each peak was integrated by Simpson's rule<sup>9</sup>, with the peak "beginning" being taken at  $\gamma = 0$ , and the peak "end" being chosen as the point where the concentration fell below a threshold of  $10^{-8}$  times the peak maximum. The integrated mass was then subtracted from unity to yield the correct split peak mass. In all, 840 theoretical peaks were generated by using all possible combinations of the following chromatographic parameters:

$$\begin{aligned} k' &= 1.0, 2.0, 4.0, 8.0, 12.0, 16.0, 20.0 \\ \gamma &= 0.001, 0.002, 0.005, 0.01, 0.02, 0.05, 0.10, 0.20, 0.50, 1.0 \\ KC_0 &= 0, 0.01, 0.02, 0.05, 0.10, 0.20, 0.50, 1.0, 2.0, 5.0, 10.0, 20.0 \end{aligned}$$

In the second set of computer simulations, target values of the split peak mass were selected (*e.g.*, 10% of the solute mass), and the results of the first simulation were used to predict which chromatographic parameters would yield the desired result. The parameter space was then searched until the targeted split peak mass was bracketed, whereupon a parabolic interpolation was performed in order to find the parameters which yielded the desired target value. The resulting parameters were then checked in eqn. 1, and if the split peak mass was not within 0.2% of the target value, the above procedure was repeated until this condition was met. By this method, 41 distinct parameter sets were obtained for each of the following split peak fractions: 1%, 2%, 5%, 10%, 20%, 30%, and 40%. The peak integration procedure used in the first set of simulations was also used in this set.

All computations were carried out in double-precision Pascal on a Zenith-151 microcomputer equipped with an 8087 coprocessor.

## RESULTS AND DISCUSSION

In order to interpret the theoretical results generated by the first set of simulations, it is convenient to introduce two dimensionless groups:

$$\theta_1 = \gamma k' = k_a S_0 \epsilon t_0 \quad (4a)$$

$$\theta_2 = \gamma KC_0 = k_a C_0 t_0 \quad (4b)$$

Of the 840 peaks generated in the first set of simulations, there were only 573 unique combinations of  $\theta_1$  and  $\theta_2$ . For those peaks which had identical values of  $\theta_1$  and  $\theta_2$ , but entirely different values of  $\gamma$ ,  $k'$ , and  $KC_0$ , the retained peak profiles differed widely in shape and breath—but the split peak mass was identical to at least fourteen significant figures. This observation validates our computational procedure, because neither  $\theta_1$  nor  $\theta_2$  are dependent upon  $k_d$ . The split peak effect must be independent of  $k_d$ , for its size depends only on the probability of a solute *adsorbing*; the probability of it *desorbing* is completely irrelevant to the size of the peak eluting at the dead volume. It therefore follows that the split peak effect can be completely described by the two

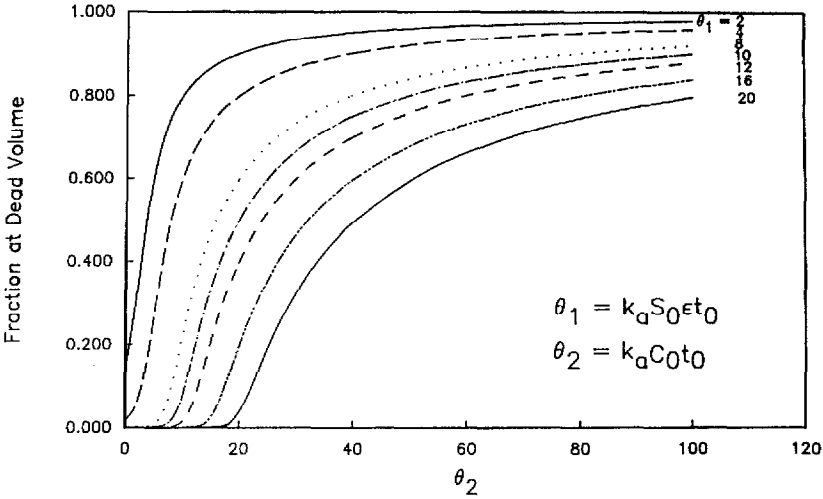


Fig. 1. Fraction of solute eluting at the dead volume as a function of both  $\theta_1$  and  $\theta_2$ .

parameters,  $\theta_1$  and  $\theta_2$ , which incorporate slow chemical adsorption (via  $k_a$ ), the concentration of binding sites ( $S_0\epsilon$ ), the flow-rate (through  $t_0$ ), and the solute load ( $C_0$ ). Some of the data that were generated in the first set of simulations are presented in Fig. 1, and in alternative form in Fig. 2. Several features of these plots are instructive. First, the data plotted in Fig. 2 yield a plot which is virtually identical to one generated by Hage and Walters<sup>5</sup> from numerical simulations. The slopes of all the lines in Fig. 2 are equal to unity at small values of  $\theta_1$ , while at large values, the lines become substantially curved. Again, these patterns in the data are identical to those found in the numerical work of Hage and Walters<sup>5</sup>.

From Figs. 1 and 2, it is evident that the split peak mass, or fraction of solute eluting at the dead volume, is a very complex, non-linear function of  $\theta_1$  and  $\theta_2$ . Herein lies the difficulty of using split peak theory to measure  $\theta_1$  and  $\theta_2$  experimentally, and

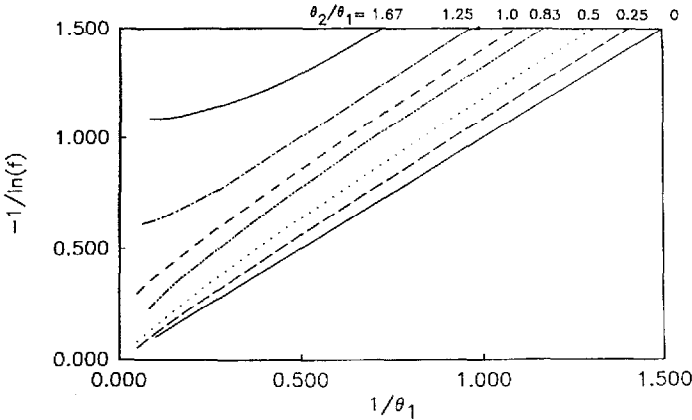


Fig. 2. Data from Fig. 1 plotted in alternative form to maintain consistency with ref. 5.

thereby obtain  $k_a$  and  $S_0$ . Simultaneous measurement of these parameters would require a series of experiments in which  $\theta_1$  and/or  $\theta_2$  were varied, and experimental plots similar to Figs. 1 or 2 constructed. Lengthy and involved computer computations would then be required to match a theoretical working curve to the experimental curve. Alternatively, the binding site concentration can be measured independently by chemical means, and then split peak behavior can be extrapolated to infinite dilution to yield  $k_a$ ; this has been the method employed by Hage and co-workers<sup>3,5</sup>.

Another way of measuring these parameters is to fit retained peaks (or breakthrough curves) to theoretical profiles<sup>6,10-13</sup>. This method has two principal advantages. First, all three parameters ( $k_a$ ,  $k_d$ , and  $S_0$ ) are accessible, as opposed to just two ( $k_a$  and  $S_0$ ); secondly, these parameters may be obtained simultaneously from *each* chromatogram. Multiple runs, while desirable for assessing the precision and accuracy of the method, are not necessary for the actual measurement of the parameters. In addition, there are practical reasons why the curve-fitting approach is to be preferred. The computations involved in the data analysis are no worse—and may even be less involved—than those required to fit working curves to experimental split peak plots. Also, the split peak method requires that a peak at the dead volume be accurately integrated; this requires that there be no unusual dead volume effects or unretained components that interfere with the split itself, and that the detector responds quickly enough.

In preparative separations, the split peak effect is obviously an undesirable artifact. In an affinity chromatographic separation, for instance, a split peak would mean that a portion of the desired product would elute in the wash along with other unretained (and undesired) components. It is therefore important to have a fundamental understanding of how the effect may be controlled, even if it is not possible—or practical—to use it in making physico-chemical measurements. For the purpose of optimizing solute throughput in a new affinity system, such as that recently reported by Hage and Walters<sup>14</sup>, it would be useful to understand how throughput is related to the fraction of unretained solute. If the throughput is taken to be the ratio  $C_0/t_0$ , then from eqns. 4a and 4b, we may define a dimensionless throughput parameter:

$$\text{TP} = \frac{\theta_2}{\theta_1^2} = \frac{C_0}{k_a(S_0\varepsilon)^2 t_0} \quad (5)$$

The second set of simulations is summarized in Fig. 3. The region below each curve represents all combinations of  $\theta_1$  and  $\theta_2$  where the split peak fraction is *less than* the percentage indicated on the graph. The accuracy of these plots rests upon the assumption that chemical processes are slow relative to mass transfer, and upon prior knowledge of  $k_a$  and  $S_0$ . If these parameters have been accurately determined by alternative means, then plots such as those depicted in Fig. 3 may be used to adjust  $t_0$  (via the flow-rate) and  $C_0$  (the solute load) to achieve optimum solute throughput at a given split peak fraction.

At large values of  $\theta_1$ , all of the curves in Fig. 3 approach a straight line with a limiting slope which is greater than unity. If a small split peak fraction is specified (e.g., 1%) this slope is very close to unity, while for large split fractions (e.g., 40%), the slope is much larger (close to 2 in the latter case). It must be remembered that both  $\theta_1$  and  $\theta_2$  are proportional to  $t_0$ , the dead time of the column. This means that an

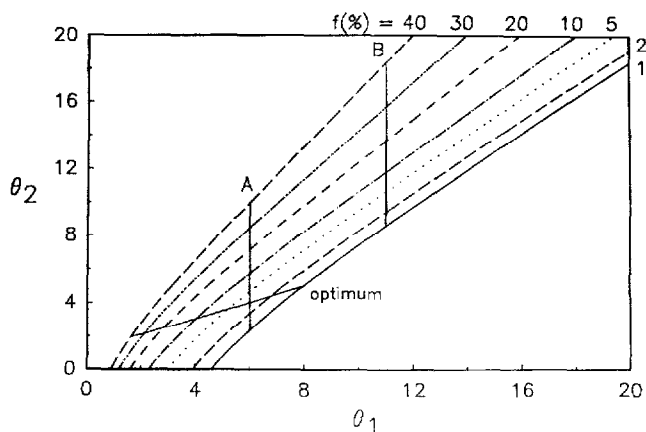


Fig. 3. Selected values of the split peak fraction, and the parameter values which give these fractions. The intersection of the optimum line with the curves represents the point of optimal solute throughput for a specified fraction. See text for details.

experimental point on any curve in Fig. 3 would move along a line with slope equal to unity as the flow-rate is changed. A point that was on, say, the 1% line would then find itself slightly above the line after a flow-rate increase; that is, the split peak fraction would be greater than the desired amount. A downward adjustment in the solute load ( $C_0$  in  $\theta_2$ ) would then be required to bring the point back onto the curve. In general, the smaller the split peak fraction that is specified, the less will  $C_0$  need downward adjustment to compensate for a flow-rate increase.

This raises the question as to how to adjust the sample load and flow-rate to achieve the maximum separation productivity. To find the optimum throughput for each of the indicated split peak fractions in Fig. 3, eqn. 5 was used to compute the dimensionless throughput for each of the 41 points on each curve. A distinct maximum was found on each curve; it was pinpointed by means of a parabolic interpolation between the three points with the highest throughput. The optimum points on each curve are given in Table I, and are connected in Fig. 3 with the solid curve labeled "optimum".

TABLE I

VALUES OF  $\theta_1$  AND  $\theta_2$  REQUIRED TO ACHIEVE THE MAXIMUM POSSIBLE SOLUTE THROUGHPUT AT VARIOUS SPLIT PEAK FRACTIONS

$f(\%)$	$\theta_1(opt)$	$\theta_2(opt)$	$TP^*$	$(1-f)TP$
1.00	7.945	4.975	0.0788	0.0780
2.00	6.762	4.383	0.0959	0.0940
5.00	5.203	3.608	0.1333	0.1266
10.0	4.025	3.038	0.1875	0.1688
20.0	2.834	2.478	0.3085	0.2468
30.0	2.126	2.153	0.4762	0.3333
40.0	1.628	1.947	0.7342	0.4405

\*  $TP$  is the dimensionless solute throughput defined in eqn. 5.

TABLE II  
NET THROUGHPUT AS A FUNCTION OF SOLUTE LOAD

Flow-rate is constant.

Line*	$f$ (%)	$TP$	$(1 - f)TP$
A	1.00	0.0657	0.0650
	10.0	0.1597	0.1438
	40.0	0.2769	0.1662
B	1.00	0.0710	0.0703
	10.0	0.0977	0.0879
	40.0	0.1518	0.0911

\* Refer to Fig. 3.

Two observations need to be made regarding the data in Table I. First, the points of optimum throughput for the chosen split peak fractions lie on an almost perfect line ( $r = 0.9997879$ ). It would therefore be possible to estimate the optimum flow-rate and sample load for *any* desired split fraction in the range 1 to 40%, provided that the physico-chemical parameters of the system were known. The last column in Table I is also interesting; it suggests that net throughput can be improved by simply tolerating more split peak mass, and adjusting the operating parameters to the optimum point. This observation is borne out by the data in Table II, which shows that increasing the sample load increases the net throughput—regardless of the concomitant increase in the split peak fraction. The improvement in net throughput, however, is much less for larger values of  $\theta_1$  (line B in Fig. 3).

## CONCLUSIONS

The theory of split peak chromatography under non-linear conditions has been discussed, and the behavior of split peaks over a wide variety of experimental conditions has been described. The computations pertain only to the case where mass transfer is fast relative to chemical sorption processes. While not ideal for making physico-chemical measurements, non-linear split peak theory may be useful in making separation design calculations—provided that the physical parameters of a chromatographic system have been accurately measured by alternative means. Universal working curves and tabular data are presented which quantitatively describe how, for a specified split fraction, solute throughput may be optimized by adjusting the flow-rate and solute load to an optimal point. In maximizing solute throughput, it is advantageous to tolerate a greater split peak fraction, while adjusting operating parameters to the computed optimum.

## LIST OF SYMBOLS

- $C_0$  quantity of solute injected in a very high, narrow pulse =  $C_p(V_p/V_0)$ ;  
 $C_p$  concentration of solute in the very narrow injection pulse;  
 $f$  fraction of the solute mass eluting at the dead volume;



- $I_0(x)$  zeroth order Bessel function of the first kind;  
 $I_1(x)$  first order Bessel function of the first kind;  
 $K$  equilibrium constant =  $k_a/k_d$ ;  
 $k'$  thermodynamic capacity factor =  $KS_0\varepsilon$ ;  
 $k_a$  second order rate constant for chemical adsorption;  
 $k_d$  first order rate constant for chemical desorption;  
 $q$  concentration of solute on the stationary phase;  
 $S_0$  concentration of active binding sites on the adsorbent surface. This is related to the surface coverage by<sup>6</sup>:

$$S_0 = \frac{A_0\rho a_s}{(1 - \varepsilon_T)}$$

where  $A_0$  is the surface coverage of sites (mol/m<sup>2</sup>),  $\rho$  is the density of the adsorbent,  $a_s$  is the specific surface area, and  $\varepsilon_T$  is the total porosity of the adsorbent<sup>6</sup>;

- $T(u, v)$  Bessel function integral which varies between zero and unity. Evaluation of this function is discussed in ref. 6;  
 $t_0$  dead time of the column (passage time of an unretained solute which can, and does, explore the pores of the adsorbent);  
 $TP$  dimensionless throughput (eqn. 5);  
 $V_0$  dead volume of the column;  
 $V_p$  volume of the pulse injected onto the column;  
 $y$  "shifted" time in dimensionless form =  $t/t_0 - 1$ ;  
 $\gamma$  dimensionless rate parameter =  $k_d t_0$ ;  
 $\varepsilon$  porosity ratio =  $(1 - \varepsilon_T)/\varepsilon_T$ ;  
 $\theta_1$  dimensionless capacity parameter for split peak work =  $k_a S_0 \varepsilon t_0$ ;  
 $\theta_2$  dimensionless loading parameter for split peak work =  $k_a C_0 t_0$ .

#### ACKNOWLEDGEMENTS

This work was supported by a grant from the Bio-Process Technology Center of the University of Minnesota. The authors also thank David Hage for advance copies of his publications, and his helpful comments.

#### REFERENCES

- 1 J. C. Giddings and H. Eyring, *J. Phys. Chem.*, 59 (1955) 416.
- 2 J. R. Sportsman and G. S. Wilson, *Anal. Chem.*, 52 (1980) 2013.
- 3 D. S. Hage, R. R. Walters and H. W. Hethcote, *Anal. Chem.*, 58 (1986) 274.
- 4 C. DeLisi, H. W. Hethcote and J. W. Brettler, *J. Chromatogr.*, 240 (1982) 283.
- 5 D. S. Hage and R. R. Walters, *J. Chromatogr.*, 436 (1988) 111.
- 6 J. L. Wade, A. F. Bergold and P. W. Carr, *Anal. Chem.*, 59 (1987) 1286.
- 7 H. C. Thomas, *J. Am. Chem. Soc.*, 66 (1944) 1664.
- 8 H. C. Thomas, *Ann. NY Acad. Sci.*, 49 (1948) 161.
- 9 R. L. Burden, J. D. Faires and A. C. Reynolds, *Numerical Analysis*, PWS Publishers, Boston, MA, 1981, p. 142.
- 10 F. H. Arnold and H. W. Blanch, *J. Chromatogr.*, 355 (1986) 13.
- 11 F. H. Arnold, H. W. Blanch and C. R. Wilke, *Chem. Eng. J.*, 30 (1985) B9.
- 12 H. A. Chase, *J. Chromatogr.*, 297 (1984) 179.
- 13 H. A. Chase, *Chem. Eng. Sci.*, 39 (1984) 1099.
- 14 D. S. Hage and R. R. Walters, *J. Chromatogr.*, 386 (1987) 37.